LRP 385/89 August 1989

DIRECT MEASUREMENT OF ION PHASE SPACE ORBITS IN AN ELECTROSTATIC FIELD

A. Fasoli, T.N. Good, F. Anderegg, F. Skiff, P.J. Paris,
M.Q. Tran, M. Yamada

DIRECT MEASUREMENT OF ION PHASE SPACE ORBITS IN AN ELECTROSTATIC FIELD

A. Fasoli, T.N. Good, F. Anderegg[a], F. Skiff[b],
P.J. Paris, M.Q. Tran, M. Yamada[c]

Centre de Recherches en Physique des Plasmas
Association Euratom - Confédération Suisse
Ecole Polytechnique Fédérale de Lausanne
21, Av. des Bains - CH-1007 Lausanne - Switzerland

ABSTRACT

Ion orbits are followed in phase space by means of a new scheme of the optical tagging plasma diagnostic technique.

An orbit distortion for ions interacting resonantly with an Ion Acoustic wave is clearly observed even in the low excitation regime, where the plasma response and the corresponding macroscopic fields exhibit linear behavior.

(a) Present Address : Univ. of California San Diego, Dept. of Physics, La Jolla, CA 92093, U.S.A.
(b) Permanent Address : Lab. of Plasma Research, Univ. of Maryland, College Park MD 20742, U.S.A.
(c) On leave from : Plasma Physics Lab., Princeton Univ., Princeton NJ 08543, U.S.A.

Among the different levels of plasma description, the finest information is inferred from the kinetic model; however, the lack of non-perturbative diagnostic tools for measuring kinetic quantities has often prevented a complete understanding of plasma dynamics. Frequently, as in particle diffusion or heating problems, the key element of a physical effect is the transition from the single particle motion to the macroscopic mean fields via a natural ensemble integration over the phase space. This transition, which depends on the topology of the particles' phase space trajectories, determines the character of the plasma interaction with a force term (typically an electromagnetic wave), as well as the nature of possible wave or particle non-linearities and the significance of self-consistent effects. Since the fields are derived from the particle currents and densities, the particle orbits acquire a fundamental character. The main diagnostic task is then to find a correlation between successive points (p,q) in ion or electron phase space, i.e. to reconstruct the individual particle orbits by experimentally *integrating* the equation of motion. Previous efforts in measuring the electron[1] or ion[2] phase space have led to the observation of *cuts* or projections of it, by evaluating the number density versus time or, independently, the space or velocity variables.

In this Letter we report phase space trajectory measurements for spectroscopically active ions in an electrostatic field. Specifically, a method to correlate the average velocity of a class of particles along an arbitrary portion of an orbit to their final velocity is demonstrated. As an application, a distortion of the ion orbits due to grid launched ion-acoustic (IA) waves has been observed.

The experiments are performed on the Linear Magnetized Plasma (LMP) Q-device[3,4], a uniformly magnetized (B<0.3 T) barium plasma column. Temperatures are determined by the barium vapor ionizing assembly: $T_e \cong T_{i\perp} \cong 2T_{i\parallel} \cong 0.2$ eV; the density is in the 10^9-10^{10} cm^{-3} range. The potential difference between the hot plate and the plasma causes a drift v_D for the ion population of about 1.2×10^5 cm/sec. The degrees of spatial and temporal fluctuation for the B field and the plasma parameters are kept below 10^{-3} and 10^{-2}, respectively. The experimental arrangement is shown in Fig.1.

The first step to investigate ion orbits is to start a set of test particles at a certain position, without perturbing the background density. The way of selecting the particles also has to leave unaltered their dynamical features, such as charge and mass. In the experiment reported herein, we meet this requirement creating the test particles by optically pumping the spin sublevel of the ion ground state to a sublevel of the first excited state via resonant interaction between a pulsed ($\tau \approx 10$ ns, E≈5 mJ) dye laser beam and the $6_2S^{1/2} \rightarrow 6_2P^{3/2}$ quantum transition[5]. Rapid decay of the excited state redistributes the pumped ions into a multiplicity of long-lived lower level states. The combination of optical pumping and redistribution yields a depletion of the state density for the pumped spin sublevel and an enhancement of state densities of other decay product states. No particular care is taken to avoid power broadening effects, since the laser spectral width is such that no velocity selection is operated at the tagging stage. In addition, the beam is directed to the plasma through a cylindrical lens, so that the optical pumping affects all the particles belonging to a vertical section of the plasma column. The pump pulse duration is short enough to avoid

saturation effects due to finite particle transit-time across the beam[6]. The spin polarized ions are detected by observing the relative change of the fluorescence induced by a cw dye laser (the "search") tuned to the same state transition. Better S/N ratio is obtained when the *dark* signal scheme is adopted, i.e. when pump and search are performed on the same Zeeman line. Therefore, the LIF search signal shows a reduction in amplitude where and when the tagged particles arrive. The search beam is injected into the plasma column via a prism behind a fine mesh end plate and propagates parallel to the B field. Since its band width (<1 MHz) is much smaller than the thermal width of the chosen Zeeman line, the Doppler effect allows a velocity selection inside the parallel distribution function. A scanning optical carriage[7], on which an observation telescope and an optical fiber are mounted, detects the fluorescence signal and defines the z coordinate of the test particles at observation. In this way we select a "final" point on a certain ion orbit (p_f, q_f), the initial q being determined by the tag beam location.

The last physical quantity we need to establish a biunivocal relation between the two phase space points (p_i, q_i) and (p_f, q_f) is the initial momentum. This piece of information can be supplied indirectly by knowing the average velocity over the measured portion of orbit, and by eventually iterating this process over a series of subsegments back towards q_i. For a fixed tag-search distance this corresponds to the observation of the time of flight spectrum of the tagged particles, i.e. the temporal structure of the tag-induced change in the fluorescence signal. For typical experimental conditions ($\Delta z \cong$ 10cm) the signal at $v_{\|}=v_D$ will arrive about 80μs after the tag pulse, spread over a few μs mainly because of the finite tag beam size in z, the bw of the search laser being

negligible. To record these spectra, whose peak position defines the time of flight of the selected final velocity class, we apply a time resolved detection technique, using a boxcar integrator to average over several pulses of the tag laser. A special double gate arrangement for the search laser and the wave signal is needed to avoid depletion of the ion target state before the tag pulse is on, and to keep constant track of the wave phase. Two schemes for the acquisition system can be applied : to fix the final velocity by picking one laser mode frequency and observing the corresponding time-of-flight spectrum, or to choose a certain time of flight (by "holding" the boxcar time window) and to scan the laser frequency, looking for the ion class which had that particular average velocity along its orbit.

In order to have a non-trivial structure to investigate on the ion phase space, and to deal with a 1-D propagation scheme (no $k_\perp$ component) an ion-acoustic wave is excited by a grid with 3mm spacing. Damping lengths, wavelengths, and phase velocity are measured from optical interferograms[8], obtained when the cw beam is introduced perpendicular to the field, so that the LIF signal is naturally integrated over $v_{||}$. The form of the zero and first order parallel distribution functions[8] ($f^{0,1}(v_{||})$) shown in fig.2 confirms the linear character of the wave for the excitation parameters used in the experiment (f=43.5 kHz; $-5V<V_{DC}<8V$, $V_{AC}<1V$). A calibration of the kinetic perturbation via time synchronous detection, gives an evaluation of the wave amplitude in terms of $\delta n/n$, which is kept below 10%. The reversibility of the damping, and the consequent absence of dissipative collisional effects, suggested by the form of $f^1(v_{||})$ which exhibits phase mixing as the distance from the grid is increased, are confirmed by the appearance of

a plasma echo, when two waves of proper frequencies are launched at different positions[9].

The characteristics of the experimental scenario, with respect to both the diagnostics and the wave launching scheme, allow us to use a simple one-dimensional 1-particle hamiltonian model to describe the IA wave-particle interaction. Considering an ion in the damped potential of an electrostatic wave, we can write the Hamiltonian in the wave frame

$$H = \frac{p^2}{2} + e^{-(z+v\tau_0 t)/\alpha} \sin(2\pi z+\psi) \qquad (1)$$

where p is normalized to $(me\phi_0)^{1/2}$ (ϕ_0 : wave amplitude at z=0), $z = z_{real}/\lambda$ and $\alpha = d/\lambda$ is the ratio of the damping length to the wavelength. Normalizing the time to $\tau_0 = (md\lambda/e\phi_0)^{1/2} = \sqrt{\alpha}\,\tau_B$, where τ_B is the bounce time in the potential trough, we get the following equation of motion:

$$\ddot{z} = e^{-(z+v\tau_0 t)/\alpha} [\sin(2\pi z+\psi) - 2\pi\alpha \cos(2\pi z+\psi)] \ , \qquad (2)$$

whose solutions for a set of initial conditions are shown in Fig. 3, as well as the spatial form of the electrostatic wave that motivated the choice for the potential energy in (1). Despite the simplicity of the model, several physical features of the interactions can be extracted, concerning the quantitative (in terms of the RF induced difference in average velocities or times of flight) distortion of the orbits as a function of different experimental parameters.

The IA wave induced change in time of flight (ΔT) on the drifting ions is shown in fig.4a; the resonant feature of the wave-particle energy exchange arises from the form of the ΔT vs. $v_{||}^{final}$ curve, which shows a narrow peak around the $v_{||}^{final}$ value corresponding to the wave phase velocity. In Fig.4b, the time of flight results on the plane $v_{||}^{average}$-$v_{||}^{final}$ are compared to the theoretical predictions: a distortion of the straight line orbits is clearly demonstrated by a modification of the one to one ratio $v_{||}^{average}/v_{||}^{final}$.

The inherent kinetic character of the interaction, as well as the dynamical "sensitivity" of the experiment, issue from the measurements shown in Fig. 5, where the RF induced change in the time of flight is plotted versus the temporal phase (ψ) of the wave, for two velocities in the resonant interaction region. A shift in the initial wave phase, which corresponds qualitatively to a z shift in the curve of Fig. 3, implies a periodical change of ΔT, both in magnitude and sign. Note that because of the drift, the periodicity in the laboratory frame depends on the class of particles considered.

A scaling of the RF induced ΔT values as a function of the amplitude of the wave, for resonant particles, is shown in Fig. 6. A dependence on the square root of the grid potential ($V_{AC}^{1/2}$), predicted by the numerical model and by a qualitative consideration, based on the $\phi^{1/2}$ scaling of the resonant velocity region width, is shown in the log-log plot.

In summary, a complete non-perturbative reconstruction of ion orbits in phase space has been performed using a variation of the spin

state tagging technique[5]. A distortion of ion orbits around the phase velocity of an IA wave has been observed even in the parameter range where neither $f^n(v_{||})$ (n=0,1) nor the interferometric wave patterns indicate any deviation from the linear regime[10].

More generally, the power of this method lies in the fact that the macroscopic scale expansion of the plasma response in terms of the perturbation amplitude is somehow by-passed by looking directly at the particle trajectories. Several applications are suggested by the broad validity range of one-particle hamiltonian models and by the intrinsic exhibition of self-consistent effects. Of particular interest, in relation to heating and diffusion problems both in astrophysical and thermonuclear plasmas, is the experimental observation of the transition to stochasticity[11,12,13], due to the chaotic breaking up of particle orbits close to the separatrix, when more than one resonance is produced in the plasma.

This work was partially supported by the Fonds National Suisse de la Recherche Scientifique under Grants No. 20-5409-87 and 20-25526-88.

References

1 R.L.Stenzel, W.Gekelmann and N.Wild, *Phys. Fluids* **26**, 1949 (1983).
2 R.McWilliams and D.Sheehan, *Phys. Rev. Lett.* **56**, 2485 (1986).
3 M.Q.Tran et al., *CRPP Laboratory Report* LRP 205/82 (1982).
4 P.J.Paris et al., *CRPP Laboratory Report* LRP 350/88 (1988).
5 F.Skiff et al., *Phys. Lett. A* **137**, 57 (1989).
6 R.A.Stern, *Phys. Fluids* **21(8)**, 1287 (1978).
7 F.Anderegg et al., *Rev. Sci. Instrum.* **59 (10)**, 2306 (1988).

8 T.N.Good et al., *"Non linear phenomena in Vlasov Plasmas"*, p.255, F.Doveil Ed., Editions de Physique, Orsay, 1989.
9 A.Fasoli et al., *XIX International Conference on Phenomena in Ionised Gases*, Beograd, July 1989.
10 I.B.Bernstein, J.M.Greene and M.D.Kruskal, *Phys. Rev.* **105**, 546 (1957).
11 F.Skiff, F.Anderegg and M.Q.Tran, *Phys. Rev. Lett.* **58**, 1430 (1987).
12 G.R.Smith and A.N.Kaufman, *Phys. Rev. Lett.* **34**, 1613 (1975).
13 F.Skiff et al., *Phys. Rev. Lett.* **61**, 2034 (1988).

Figure captions

Fig. 1. Experimental arrangement. The tag-search distance can be varied from 0 to 150 cm. $\lambda_{tag}=\lambda_{search}=493.4$ nm. $P_{search}\approx 50$ mW.

Fig. 2. Zero and first order parallel distribution functions. $V_{DC}=-4$ V; $V_{AC}=0.4$ V; f=40 kHz; $\Delta z(tag, search)/\lambda=2.9$. The arrow indicates the position of the phase velocity.

Fig. 3. Theoretical phase space ion orbits, calculated in the wave frame from equation (2). $e\phi/kT=0.05$ at $z=2\lambda$. The zero-order ion distribution is also displayed on the normalized p_z axis, for comparison purposes. The curve underneath represents the corresponding optically measured interferometric pattern ($V_{DC}=-4$ V; $V_{AC}=0.8$ V; f=43.5 kHz, $\lambda=4.2$ cm).

Fig. 4. a): IA wave induced change in time of flight for different velocity classes. The wave parameters are the same as in Fig.3. b): correlation between the average velocity along an orbit segment and the final velocity of the ions interacting with the linear wave. A wiggle around the phase velocity is seen, as predicted by the one-particle hamiltonian model (dashed curve).

Fig. 5. IA wave induced ΔT as a function of the wave phase, for two velocity classes close to the phase velocity. In the lab frame the selected particle velocity determines the effective periodicity.

Fig. 6. Dependence of the wave induced Δt on the exciting grid voltage. $V_{DC}=-4$ V; f=43 kHZ; $\Delta z/\lambda=2.9$; the final velocity is fixed nearly at the phase velocity of the wave. The log-log representation underlines the $V^{1/2}$ dependence (continuous line).

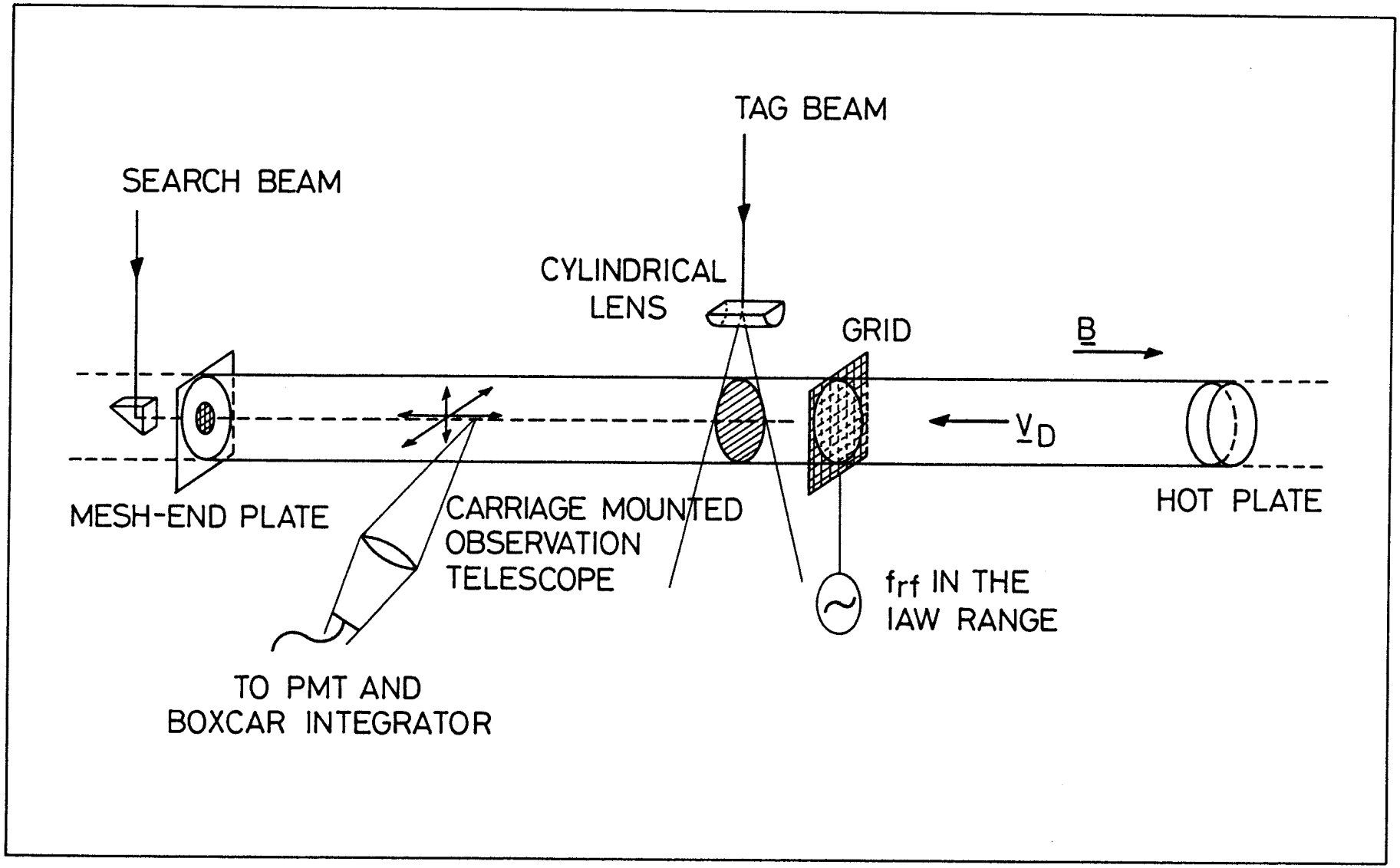
TAG BEAM
SEARCH BEAM
CYLINDRICAL
LENS
GRID
B
V_D
MESH-END PLATE
CARRIAGE MOUNTED
OBSERVATION
TELESCOPE
HOT PLATE
f_{rf} IN THE
IAW RANGE
TO PMT AND
BOXCAR INTEGRATOR

Fig. 1

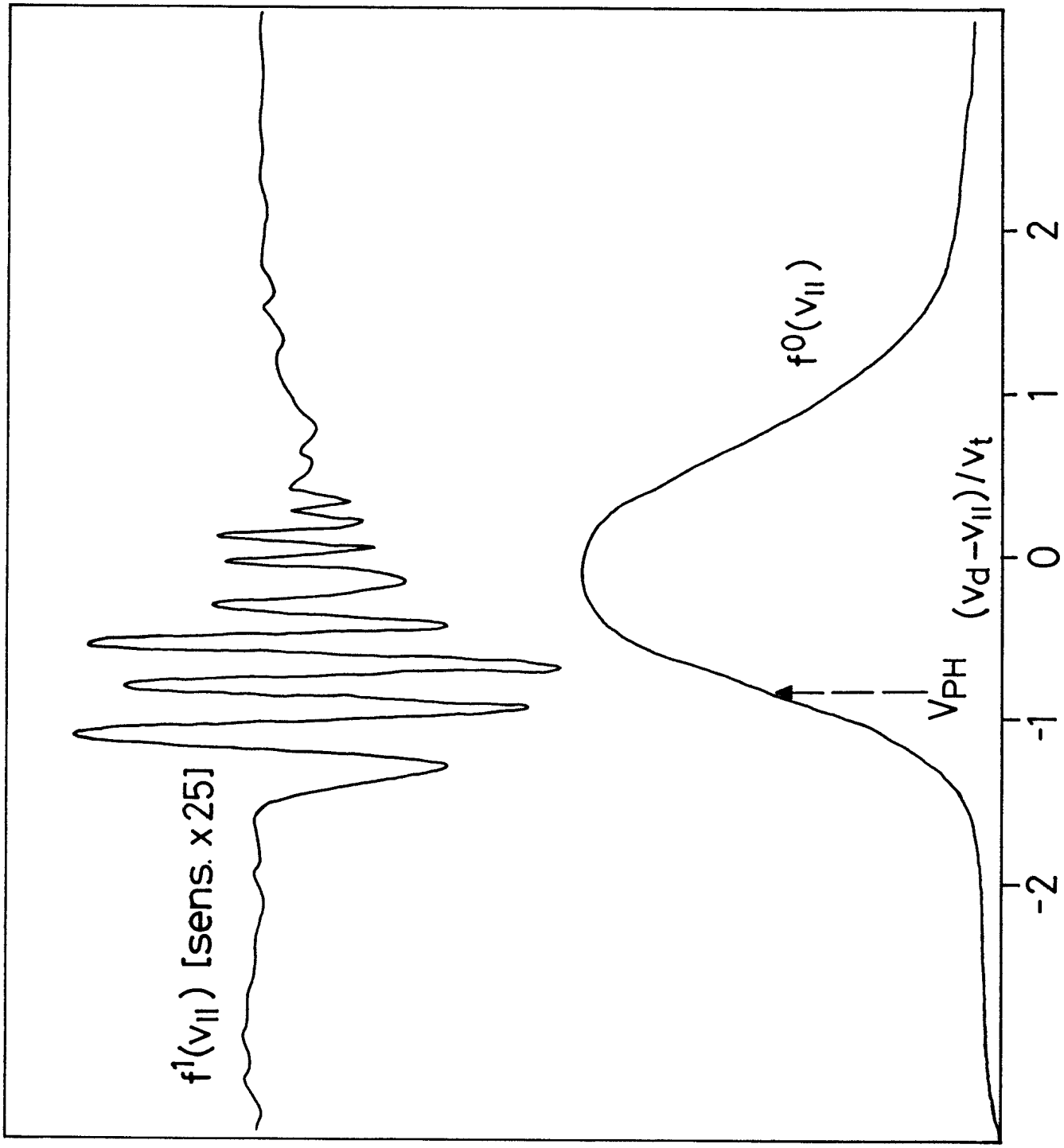

Fig. 2

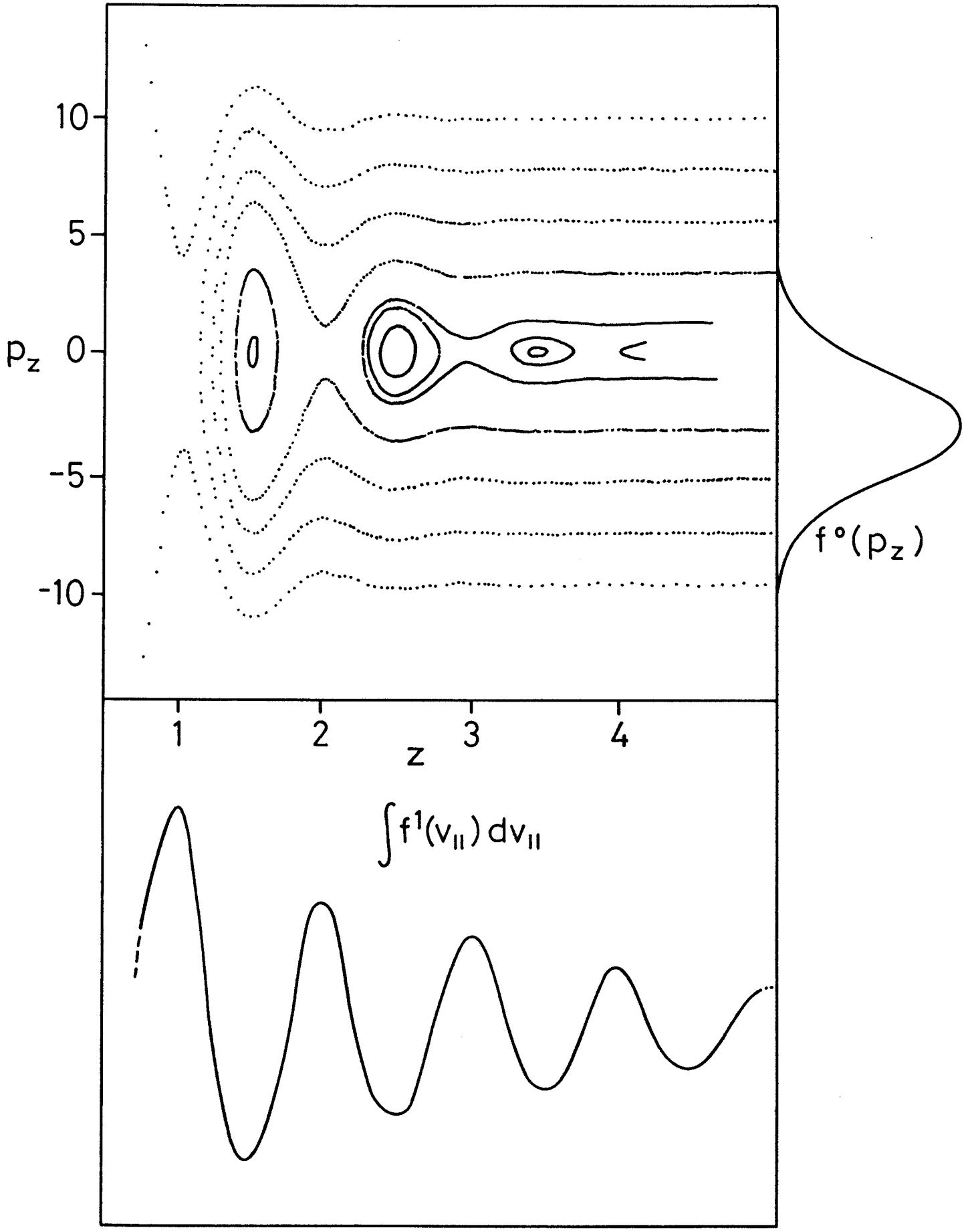

Fig. 3

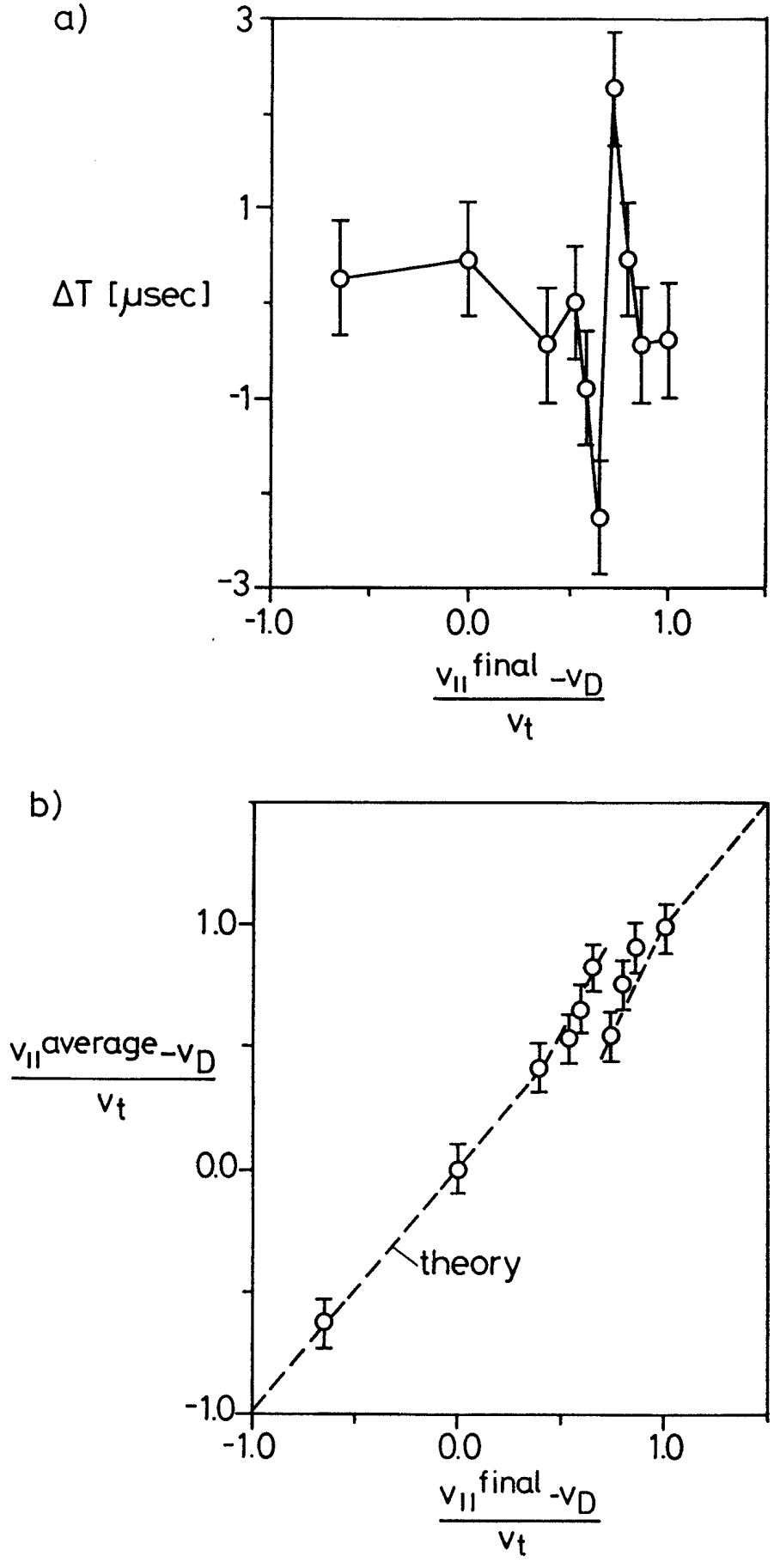
a)
3
1
-1
-3
ΔT [μsec]
-1.0
0.0
1.0
v_II final -v_D / v_t
b)
1.0
0.0
-1.0
v_II average -v_D / v_t
theory
-1.0
0.0
1.0
v_II final -v_D / v_t

Fig. 4

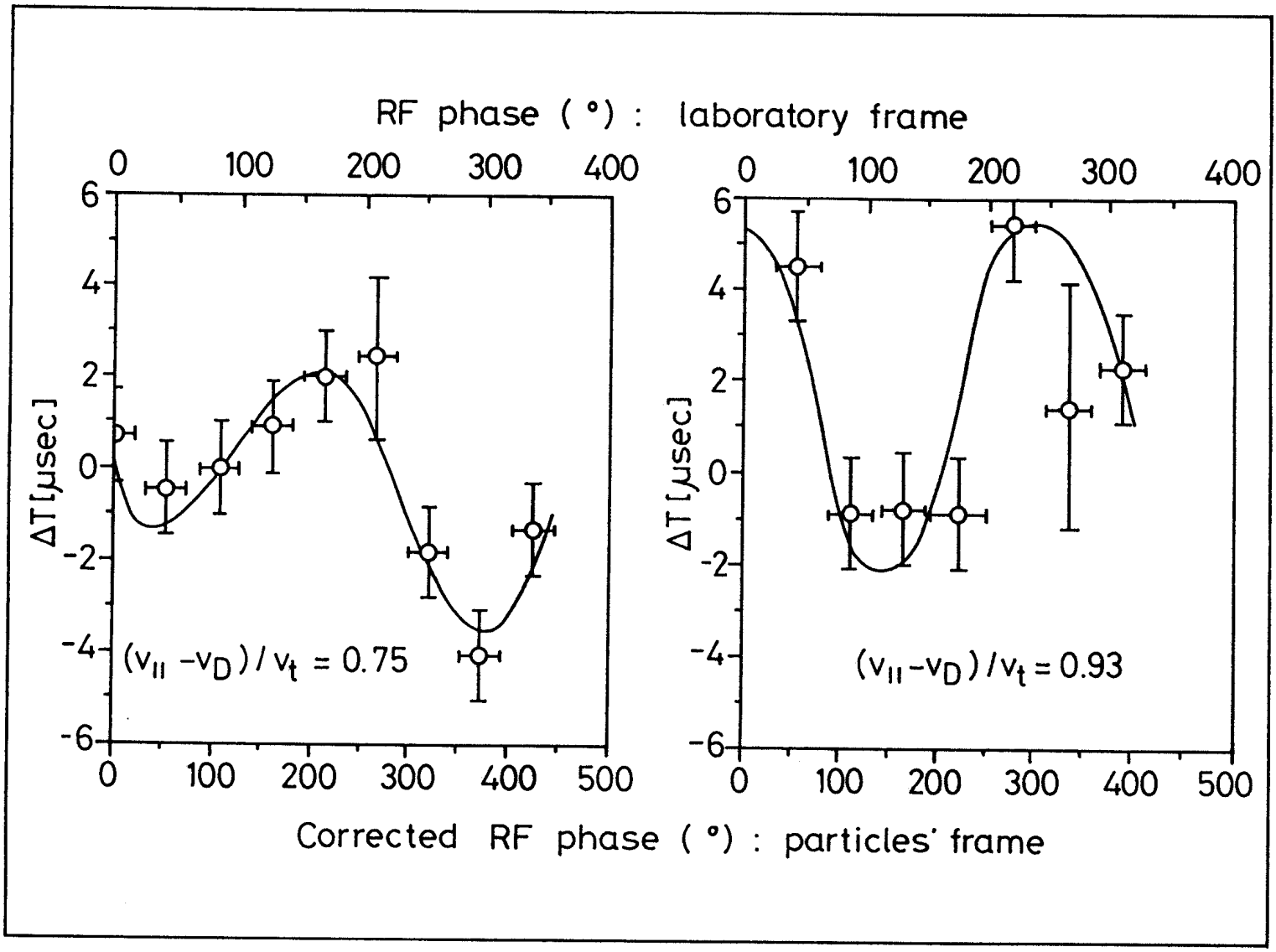
RF phase (°) : laboratory frame
0
100
200
300
400
6
4
2
0
-2
-4
-6
ΔT [μsec]
$(v_{II} - v_D) / v_t = 0.75$
$(v_{II} - v_D) / v_t = 0.93$
500
Corrected RF phase (°) : particles' frame

Fig. 5

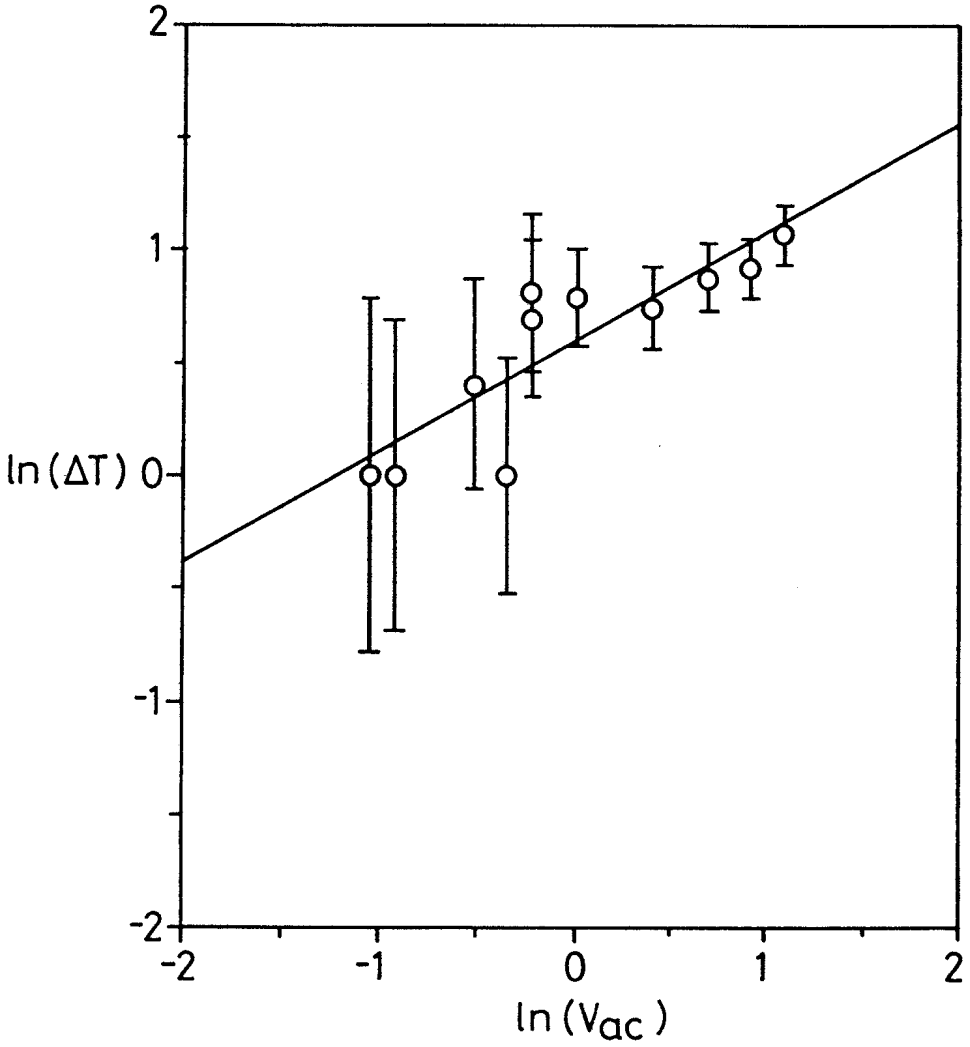

Fig. 6